Frequency Dependence of Backscatter Coefficient Versus Scatterer Volume Fraction

Jian-Feng Chen and James A. Zagzebski

Abstract— **Various groups are using the frequency dependence of backscattering to characterize tissue. In most cases, sparse scatterer concentrations are assumed in relating scattering parameters to tissue properties. This study addresses the relationship between backscatter frequency dependence and scatterer volume fraction. Backscatter coefficients (BSC) in the 2.5 to 9.0 MHz frequency range were measured for agar-gel phantoms containing Sephadex scatterers (mean diameter 42 μm) at volume fractions ranging from 5 to 50%. The BSC increased with scatterer volume fraction at low scatterer concentrations; at higher concentrations, the BSC reached a maximum with concentration and then decreased with yet increasing scatterer concentrations, as has been noted by previous authors. In addition, the volume fraction for the maximum backscatter coefficient varied with frequency, generally being greater at higher frequencies than lower frequencies, and the frequency dependence of the backscatter coefficient was greater for the higher scatterer concentrations than for the lower concentrations. These results are predicted by continuum models, where the spatial autocorrelation function depends on scatterer volume fraction.**

I. Introduction

THE frequency dependence of the backscatter coefficient is an important parameter for ultrasonic tissue characterization because it is related to the tissue microstructure [1]. For a medium containing a sparse concentration of scatterers which are spatially randomly distributed, the magnitude of the backscatter coefficient is proportional to the scatterer concentration and to fractional changes in compressibility and mass density at scattering sites. The frequency dependence of the backscatter coefficient depends primarily on the size distribution of the scatterers [2]. The variation of the backscatter signal intensity with ultrasound frequency has been used, for example, to identify dependence of dominant scatterers on ultrasound frequency in kidney examinations [3], to differentiate normal from cirrhotic liver [4], and to differentiate malignant from benign tumors in the eye [5].

Scatterers are usually grouped into one of three categories according to their size [2]. First are those referred to as specular reflectors, which have effective radii that are much larger than the acoustic wavelength. Scattering from these objects is essentially frequency independent. The second category is one for which the scattering particles are much smaller than the acoustic wavelength. These are referred to as Rayleigh scatterers. The scattered intensity from these particles varies with the fourth power of the frequency. The third case, which is between these limiting cases, is where the particle size is on the order of magnitude of the wavelength. These particles are referred to as intermediate-sized scatterers. The frequency dependence of the backscatter coefficient from these particles lies between f^0 and f^4.

When the scatterer volume fraction is high, the assumption of a random distribution of scatterers fails due to the correlation among the scatterers. The first consequence of this is that there is no longer a proportionality between the backscatter coefficient and the scatterer concentration. With red blood cells, for example, the backscatter coefficient at 7.5 MHz peaks at a hematocrit of 20%, above which it decreases with increasing hematocrit [6]. Secondly, as will be demonstrated in this paper, the frequency dependence of the backscatter coefficient changes from that for a low scatterer concentration limit, no longer depending only on scatterer size.

The topic of a backscatter frequency dependence for dense media has been treated briefly by several researchers. Morse and Ingard used a modified Gaussian spatial autocorrelation function to describe isotropic dense random scattering [7]. They found a backscatter coefficient proportional to the sixth power of the frequency for the simulated conditions. Campbell and Waag measured the backscatter coefficient versus the frequency for a medium consisting of a dense concentration of Sephadex spheres in water and found it proportional to f^5 [8]. These results are quite different from those expected (and generated experimentally) for sparse scatterer concentrations.

In this paper, the frequency dependent backscatter coefficient as a function of scatterer volume fraction is considered using continuum scattering models [9], [10]. Two models are reviewed, in which the spatial autocorrelation function describing mass density and compressibility fluctuations in the scattering medium have characteristic lengths that depend on the scatterer concentration as well as the scatterer size. These models predict a backscatter frequency dependence that varies with scatterer volume fraction. Qualitative agreement between the model predictions and experimental results are seen for Sephadex-in-agar phantoms.

II. Continuum Scattering Models

Scattering interactions in tissue may be characterized by the appropriate scattering cross section. When a transducer

Manuscript received May 31, 1994; revised December 12, 1994. This work was supported in part by a University of Wisconsin-Madison Medical Physics Department, Richard B. Mazess Advanced Fellowship, and by NIH Grant R01-CA39224.

J.-F. Chen was with the Department of Medical Physics, University of Wisconsin-Madison, Madison, WI 53706 USA. He is now with Siemens Medical Systems, Inc., Issaquah, WA 98027-7002 USA.

J. A. Zagzebski is with the Department of Medical Physics, University of Wisconsin-Madison, Madison, WI 53706 USA (e-mail: jimzag@macc.wisc.edu).

Publisher Item Identifier S 0885-3010(96)03536-8.

operating in a pulse–echo mode is placed far from a scattering volume, a fraction of the total scattered power is received by this transducer. The relevant measure is the backscatter coefficient, which is defined as the differential scattering cross section per unit volume per unit solid angle at an angle of 180°. For a continuum scattering model, the backscatter coefficient, $\eta(k)$, may be expressed as [2]

$$\eta(k) = \frac{k^4\langle\gamma^2\rangle}{16\pi^2}\iiint d(\Delta\vec{r})b(\Delta\vec{r})e^{-i\vec{k}\cdot\Delta\vec{r}} \tag{1}$$

where $k = \omega/c$ is the wavenumber, ω is the angular frequency, and c is the speed of sound in the medium. $\langle\gamma^2\rangle$ is the mean-square fluctuation of the parameter γ, which is related to the scattering strength of the random medium (see below), and $b(\Delta\vec{r})$ is the normalized spatial autocorrelation function for the medium. We will assume that the medium is isotropic so that we need consider only the magnitude of $\Delta\vec{r}$ in the spatial autocorrelation function, i.e., we can replace $b(\Delta\vec{r})$ with $b(\Delta r)$.

The medium parameter $\gamma(\vec{r})$ depends on the fluctuations in mass density and compressibility in the medium. It is expressed as [2]

$$\gamma(\vec{r}) = \gamma_\kappa(\vec{r}) - \gamma_\rho(\vec{r}) \tag{2}$$

where $\gamma_\kappa(\vec{r})$ and $\gamma_\rho(\vec{r})$ are given by

$$\gamma_\kappa(\vec{r}) \equiv \frac{\kappa(\vec{r}) - \langle\kappa\rangle}{\langle\kappa\rangle}$$

and

$$\gamma_\rho(\vec{r}) \equiv \frac{\rho(\vec{r}) - \langle\rho\rangle}{\rho(\vec{r})}.$$

The quantities $\kappa(\vec{r})$ and $\rho(\vec{r})$ are, respectively, the compressibility and the density of the medium at location $\vec{r}$. $\langle\kappa\rangle$ and $\langle\rho\rangle$ are the corresponding mean values.

Let us assume the scattering medium is a mixture of two materials, such as scattering particles in a gel background. If H represents the scatterer volume fraction in the medium, we have

$$\langle\kappa\rangle = \kappa_0 + H\Delta_\kappa \tag{3}$$

and

$$\langle\rho\rangle = \rho_0 + H\Delta_\rho \tag{4}$$

where $\Delta_\kappa = \kappa_1 - \kappa_0$, $\Delta_\rho = \rho_1 - \rho_0$ and 0 and 1 refer to the background material and the scatterers, respectively. Then, the variance of $\gamma(\vec{r})$ is given by [9]

$$\langle\gamma^2(\vec{r})\rangle \approx H(1-H)\left(\frac{\Delta_\kappa}{\langle\kappa\rangle} - \frac{\Delta_\rho}{\langle\rho\rangle}\right)^2. \tag{5}$$

In general, the spatial autocorrelation function, $b(\Delta r)$, describes the similarity of the mass density and compressibility at two positions in the scattering volume separated by the distance Δr. It was shown by Debye that for the case of a distribution of scatterers with random sizes and shapes, the scattering can be approximately characterized by an exponential autocorrelation function. For a simple two-component medium, Debye's spatial autocorrelation function can be written as (see the Appendix)

$$b_d(\Delta r) = e^{-3\Delta r/[4r_d(1-H)]} \tag{6}$$

where r_d is the characteristic radius of the scatterers in Debye's model.

A more complete model for the spatial autocorrelation function was proposed by Yagi [10]. In Yagi's model, the spatial autocorrelation function for a two-component medium is represented by the sum of two exponential terms (see (A-21) in the Appendix)

$$b_y(\Delta r) \approx 0.40e^{-\frac{\Delta r}{0.53(1-H)r_y}} + 0.60e^{-\left(\frac{\Delta r}{0.92(1-H)r_y}\right)^2} \tag{7}$$

where r_y is the characteristic radius of scatterers in Yagi's model.

The backscatter coefficient is determined by taking the Fourier transform of the spatial autocorrelation function, $b(\Delta r)$ [2]. For example, for Yagi's model, the backscatter coefficient is given by [10]

$$\begin{aligned}\eta_y(k,H) &\approx \frac{k^4 r_y^3}{12\pi}\left(\frac{\Delta_\kappa}{\kappa} - \frac{\Delta_\rho}{\rho}\right)^2 H(1-H)^4 \\ &\quad\times\left\{\frac{0.37}{[1+1.1k^2r_y^2(1-H)^2]^2} + 0.63e^{-0.85k^2r_y^2(1-H)^2}\right\}.\end{aligned} \tag{8}$$

This is identical to Mo and Cobbold's results [12]. A similar expression is obtained when the Debye autocorrelation function and correlation length are applied. Note, r_d and r_y are generally not the same value; this phenomenon is also discussed in [2].

As an example, calculations of the backscatter coefficient were performed for a simple mixture of Sephadex spheres in gel, analogous to Campbell and Waag's experimental conditions [8]. In these calculations, we assumed $r_y = 21$ μm. The term in (8) in brackets involving $(\Delta_\kappa/\kappa - \Delta_\rho/\rho)$ was set to a constant for each calculation. Figs. 1 and 2 illustrate the results of Yagi's model, both for the relative backscatter coefficient versus scatterer volume fraction and for the relative backscatter coefficient versus frequency. In Fig. 1, the results for each frequency are normalized to the maximum value of the backscatter coefficient. In Fig. 2, the backscatter coefficients at that frequency for each scatterer volume fraction are relative to the values at 2.1 MHz. At low scatterer volume fractions, the model predicts the backscatter coefficient is proportional to the scatterer volume fraction. The backscatter coefficient reaches a peak value, typically near a scatterer volume fraction of 20%, above which it decreases with increasing scatterer concentration. The interesting facet of these model predictions is that the volume fraction for the peak value should increase with increasing ultrasonic frequency. At 7.5 MHz, the peak backscatter occurs at a concentration of 25–28%, whereas the peak backscatter at 2.5 MHz occurs around a volume fraction of 18%.

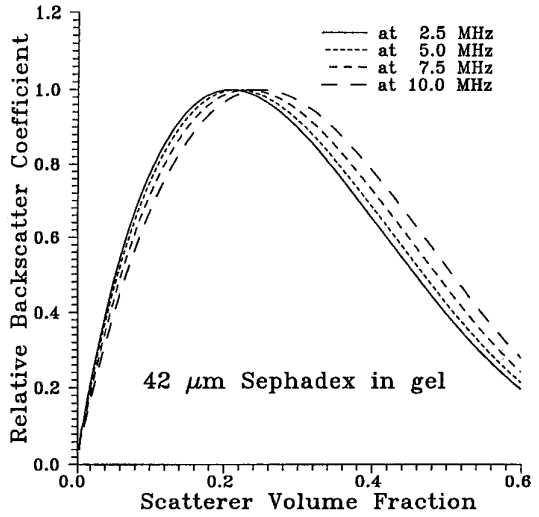

Fig. 1. Theoretical results of the backscatter coefficient as a function of scatterer volume fraction at specific ultrasound frequencies, calculated using (8). The effective scatterer diameter is assumed to be 42 μm. The results show that the peak of the backscatter coefficient moves to higher scatterer volume fractions when the ultrasound frequency is increased.

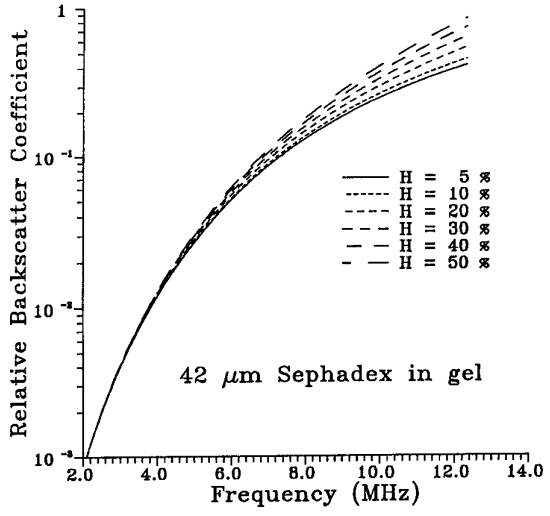

Fig. 2. Theoretical results of the backscatter coefficient as a function of ultrasound frequency, calculated using (8). The effective diameter assumed is 42 μm.

Fig. 2 shows the results of relative backscatter coefficient versus the ultrasonic frequency. The model predicts that the backscatter coefficient increases with increasing frequency faster for a medium with a high scatterer volume fraction than for a medium with a low scatterer volume fraction.

III. Experimental Methods

Several tissue mimicking phantoms were used to measure the backscatter coefficient versus the ultrasound frequency for different scatterer volume fractions and to probe further the predictions suggested by these continuum scattering models. The phantoms have identical scatterers but have different scatterer concentrations, the scatterer volume fractions ranging

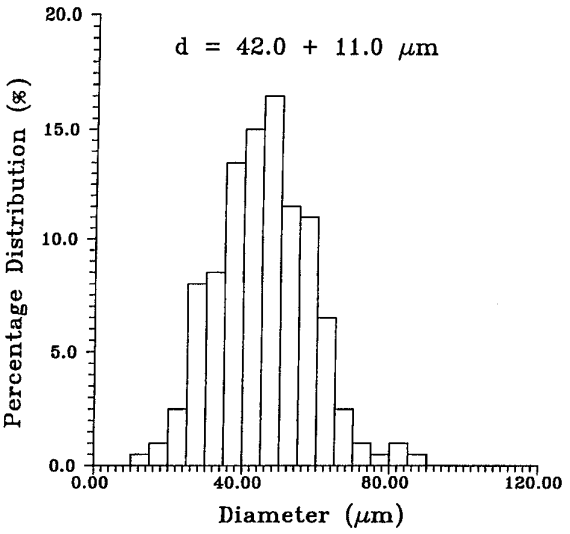

Fig. 3. Histogram showing the diameter distribution of the Sephadex particles in the test phantoms. The mean diameter is 42 μm.

from 5 to 50%. Scatterers in the phantoms are Sephadex spheres immersed in gel. The gel was congealed in 3-cm long cylinders. The two parallel surfaces of the phantoms were covered with 50-μm-thick Saran Wrap "windows" that allowed for transmission of acoustic waves. The cylinders were filled through a 2.0-cm diameter syringe epoxied into the plastic wall. After the gel solidified, the syringe was removed and the cylinder sealed.

The contents of the syringe were then extracted and sliced into 1-mm sections. An optical microscope was used to measure the diameters of scatterer in the sliced sections. The diameter distribution, shown in Fig. 3, is strongly peaked at 42.0 μm; the standard deviation of the diameter distribution is 11 μm.

The attenuation coefficients in these phantoms were measured using a narrow-band substitution method at multiple frequencies [13]. Results are shown in Fig. 4. The experimentally determined attenuation coefficients were fit using a polynomial curve of the form $\alpha(f) \approx \alpha_0 + \alpha_1 f + \alpha_2 f^2$, where $\alpha(f)$ is the curve fit attenuation, α_0, α_1, and α_2 are polynomial fitting constants, and f is the frequency in MHz. The polynomial fitting constants and the speeds of sound in all six phantoms are given in Table I.

Backscatter coefficients in the samples were measured using a broad-band as well as a narrow-band method. In both methods, echo signals from a planar reference reflector are used to derive system dependent parameters [14], [15]. For the broad-band method, a 3.5-MHz center frequency transducer was used to measure backscatter coefficients from 2 to 5 MHz. Several transducers were used to span the 2–9 MHz frequency range for the narrow-band method. Geometric parameters for these transducers are given in Table II.

Samples were placed in water in the focal region of the transducer. Broad-band excitation consisted of applying a one-cycle 3.5-MHz center frequency truncated sine wave; narrow-band excitation used an eight-cycle truncated sine wave at the frequency of interest. Time domain echo signals

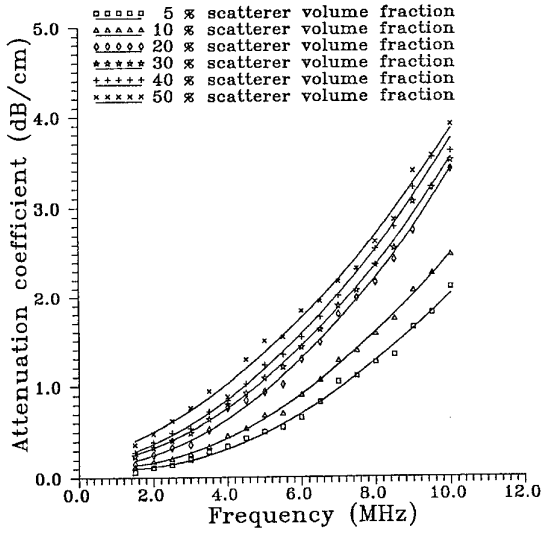

Fig. 4. Attenuation coefficients versus frequency in the test phantoms. Solid lines are the result of polynomial curve fits to the function $\alpha(f) = \alpha_0 + \alpha_1 f + \alpha_2 f^2$, where α_0, α_1, and α_2 are the fitting constants and f is the ultrasonic frequency in MHz.

TABLE I
ULTRASONIC PROPERTIES OF THE PHANTOMS USED TO STUDY BACKSCATTER COEFFICIENT VERSUS SCATTERER VOLUME FRACTION. THE ATTENUATION COEFFICIENT IS DESCRIBED IN TERMS OF CONSTANTS α_0, α_1, AND α_2, CORRESPONDING TO A SECOND-ORDER POLYNOMIAL CURVE FITTING TO EXPERIMENTAL VALUES, ASSUMING THE FORM $\alpha(f) = \alpha_0 + \alpha_1 f + \alpha_2 f^2$, WHERE f IS THE FREQUENCY IN MHZ

Phantom (% Sephadex)	α_o (dB/cm)	α_1 (dB/cm-MHz)	α_2 (dB/cm-MHz^2)	Speed of Sound (m/s)
5 %	0.1067	-0.0428	0.0235	1556±1
10 %	0.1169	-0.0280	0.0266	1563±1
20 %	0.1191	-0.0032	0.0332	1566±1
30 %	0.1410	0.0305	0.0308	1580±1
40 %	0.1324	0.0583	0.0303	1581±1
50 %	0.1949	0.1005	0.0265	1592±1

were truncated using a 10.0-μs rectangular gate for the broad-band method and a 5.0-μs rectangular gate for the narrow-band method, recorded on a digital oscilloscope (LeCroy 9400) and stored in a PC for off-line analysis. For each transducer and phantom, echo signals were recorded for 98 statistically independent locations, realized by translating the sample perpendicularly to the transducer axis. The translation steps were larger than the full width at half-maximum (FWHM) of the ultrasonic beam, assuring statistically independent echo signals. Discrete Fourier transforms of each echo signal waveform were computed. Then, the backscatter coefficients were determined using previously described methods [14], [15].

IV. RESULTS

Figs. 5 and 6 present backscatter versus frequency results for three different scatterer volume fractions, for the broad-band and narrow-band measurements. Results are shown for scatterer volume fractions of 5% (middle curve in both figures), 20% (upper curves), and 50%. As both figures indicate, the backscatter coefficient for the 50% scatterer volume fraction is actually lower than at 5%.

TABLE II
VALUES OF THE RADIUS OF CURVATURE AND THE EFFECTIVE APERTURE FOR THE TRANSDUCERS USED TO RECORD ECHO DATA FROM THE PHANTOMS HAVING DIFFERENT SCATTERER NUMBER DENSITIES

Nominal resonant frequency (MHz)	Radius of Curvature (cm)	Effective Aperture (mm)
3.5	9.65±0.07	19.2±0.2
5.0	8.50± 0.06	18.6± 0.2
7.5	6.44± 0.05	14.4± 0.2
9.0	6.44±0.05	14.4± 0.2

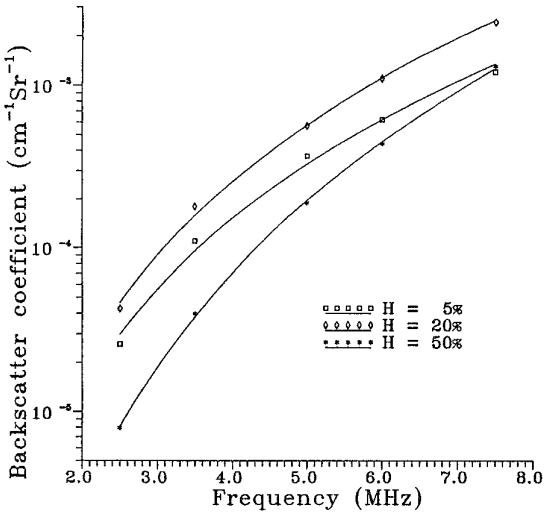

Fig. 5. Experimental results of the backscatter coefficient versus frequency for different scatterer volume fractions using the broad-band method. Dashed lines are measurement results, while the solid lines are power law fits to the measurement results. Here, the scatterer volume fraction increases from 5 to 50%.

These data exhibit a change in the frequency dependence of the backscatter for the different concentrations. For the results in Fig. 5, over the 2.5–5.0 MHz frequency range, the backscatter coefficient varies as $f^{(3.8\pm0.1)}$ for the sparse (5%) scatterer concentration sample, while for the dense (50%) sample the backscatter coefficient exhibits a $f^{(4.6\pm0.1)}$ dependence, where f is the frequency in MHz. For the narrow-band results presented in Fig. 6, over the 2.5–7.5 MHz frequency range, there is an $f^{(3.7\pm0.1)}$ dependence and $f^{(4.5\pm0.1)}$ for these two samples, respectively. (The uncertainties for the power law fit were determined using (A-24), derived in the Appendix.) The backscatter coefficients appear to exhibit a greater frequency dependence for the higher scatterer concentrations over these frequency ranges, as predicted by the continuum models.

Table III presents results for narrow-band measurements at each frequency. Column 1 gives the scatterer volume fraction,

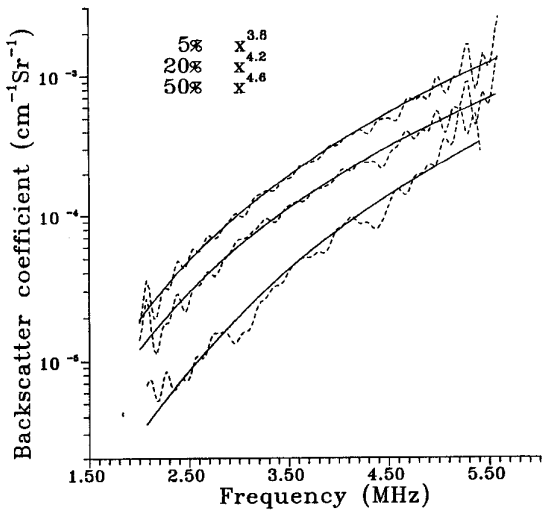

Fig. 6. Experimental results of the backscatter coefficient versus frequency for different scatterer volume fractions using the narrow-band method. Lines are power law fits to the data for the various scatterer volume fractions. Here, the scatterer volume fraction increases from 5 to 50%.

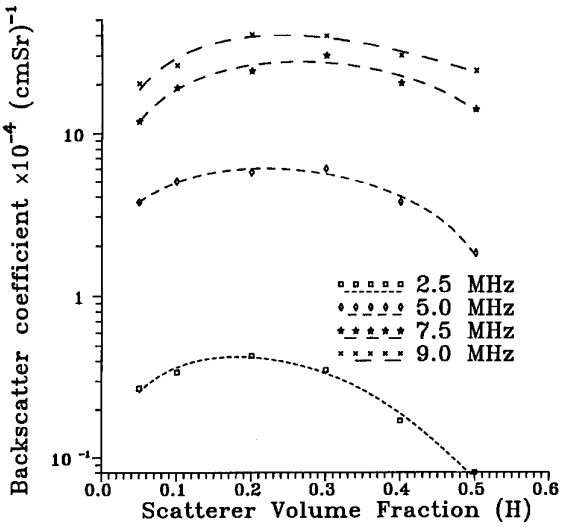

Fig. 7. Experimental results of the backscatter coefficient versus scatterer volume fraction. Dashed lines are third-order polynomial curve fits to the data for each of the four frequencies listed.

TABLE III
EXPERIMENTAL RESULTS OF THE BACKSCATTER COEFFICIENT (BSC) VERSUS SCATTERER VOLUME FRACTION AT DIFFERENT ULTRASONIC FREQUENCIES. HERE, THE BACKSCATTER COEFFICIENT IS IN UNITS OF $\times 10^{-4}(\mathrm{cm}^{-1} \cdot Sr^{-1})$

Phantoms	BSC at 2.5 MHz	BSC at 3.5 MHz	BSC at 5.0 MHz	BSC at 6.0 MHz	BSC at 7.5 MHz	BSC at 9.0 MHz
5 %	0.26±0.05	1.1±0.2	3.7±0.9	6.2±1.6	12.0±0.05	20.2±4.1
10 %	0.34±0.07	1.8±0.3	5.0±1.0	9.7±2.0	19.1±3.8	26.1±5.3
20 %	0.43±0.09	1.8±0.3	5.7±1.2	11.0±2.1	24.2±4.8	40.4±8.1
30 %	0.35±0.07	1.9±0.4	6.0±1.3	13.1±2.7	30.1±6.1	39.5±7.9
40 %	0.17±0.03	0.9±0.2	3.7±0.9	7.8±1.8	20.3±4.1	30.0±6.0
50 %	0.08±0.02	0.4±0.1	1.9±0.4	4.4±1.1	14.1±2.9	24.1±4.8

TABLE IV
THE SQUARE OF THE REGRESSION COEFFICIENT R^2 FOR THE THIRD-ORDER POLYNOMIAL CURVE-FIT TO THE BACKSCATTER VERSUS SCATTERER VOLUME FRACTION DATA. R^2 IS SHOWN FOR EACH FREQUENCY. REGRESSION COEFFICIENTS ARE ALSO SHOWN WHEN YAGI'S MODEL IS APPLIED TO THE DATA (SECOND ROW) AND WHEN A THIRD-ORDER POLYNOMIAL IS USED TO FIT YAGI'S MODEL. WHEN $R^2 = 1$, 100% OF THE SAMPLE DATA ARE EXPLAINED BY THE FITTING-CURVE

R^2 values	2.5 MHz	3.5 MHz	5.0 MHz	6.0 MHz	7.5 MHz	9.0 MHz
third-order polynomial vs. measured	0.9844	0.9323	0.9686	0.9131	0.9165	0.9494
Yagi's model vs. measured	0.9698	0.9198	0.9155	0.8702	0.8674	0.9335
Yagi's model vs.third-order polynomial	0.9987	0.9987	0.9982	0.9998	0.9960	0.9993

TABLE V
THE THIRD-ORDER POLYNOMIAL FITTING CONSTANTS FOR THE BSC, $\eta(H) \approx \beta_0 + \beta_1 H + \beta_2 H^2 + \beta H^3$, ARE LISTED FOR EACH FREQUENCY, WHERE $H = 5$, 10, 20, 30, 40, AND 50%. ALSO LISTED IS A PEAK VALUE OBTAINED FROM DIFFERENTIATING THESE CURVES WITH RESPECT TO THE SCATTERER CONCENTRATION

Frequency (MHz)	β_0	β_1	β_2	β_3	Concentration for peak BSC
2.5	5.89×10^{-2}	4.54	-16.7	15.3	18 %
3.5	3.28×10^{-1}	19.6	-67.2	56.4	20 %
5.0	1.91	41.4	-120	72.7	22 %
6.0	2.20	94.3	-252	144	24 %
7.5	3.10	200	-465	214	26%
9.0	3.73	346	-999	776	24 %

expressed as a percentage. Columns 2 through 7 are the backscatter data for various frequencies. Errors represent ± 1 standard deviation of the data from the 98 measurements on each sample.

These data, along with third-order polynomial curve fits to the backscatter coefficients, are plotted in Fig. 7. A third-order polynomial was used because it is capable of following the anticipated dependencies of backscatter on concentration, yet it does not restrict the curve to any particular model, including those in Section II. The suitability of the curve fits was analyzed by computing regression coefficients for the plots using commercially available software (Delta Graph Version 3.5, Delta Point Inc., Monterey, CA). Regression coefficients, R^2, are presented in Table IV for the narrow-band data [16]. The fitting parameters are listed in Table V for each frequency. Also listed is a peak value obtained from differentiating these curves with respect to the scatterer concentration.

The fitted curves were normalized to their peak values and replotted in Fig. 8. The original backscatter coefficient data, also normalized to the peak values of the fitted data at each frequency, are included with these curves. The normalized curves qualitatively follow the expected backscatter versus concentration data predicted using the Yagi model; that is, the scatterer volume fraction for the maximum backscatter coefficient increases with frequency. The only exception is for the 9 MHz data, which seem to exhibit a peak in the backscatter coefficient at a lower concentration than for 7.5 MHz. At this time it is not known whether this is due to measurement uncertainties (both scatter data and attenuation

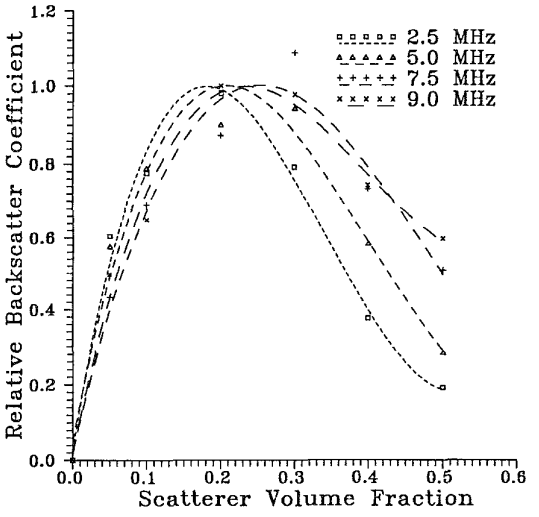

Fig. 8. Experimental results of the relative backscatter coefficient versus scatterer volume fraction. Dashed lines are third-order polynomial curve fits to the data for each of the four frequencies listed. Here, the backscatter coefficients were normalized based on their fitting curves.

data are involved), to variations during the production of the test samples, or to possible differences in the different frequency dependence of the backscatter in different frequency ranges.

V. Discussion

Generally, the maximum variation of backscatter with ultrasonic frequency expected for a medium having scatterers much smaller than the wavelength is a fourth-power frequency dependence. For the 5% scatterer volume fraction, 42-μm Sephadex spheres exhibited approximately this behavior below 5 MHz, where an $f^{3.8\pm0.1}$ frequency dependence was observed. However, the frequency dependence of scattering exceeded f^4 for a 50% scatterer volume fraction, agreeing qualitatively with Campbell and Waag's results [8]. This result is also anticipated by Mo and Cobbold [12]. As illustrated by our analysis using continuum scattering models, a greater than fourth-power frequency dependence of scattering for dense scattering media is an expected outcome when the spatial autocorrelation function in the medium has a characteristic length that is a function of the scatterer volume fraction.

Application of continuum scattering models and the resultant scatterer spatial autocorrelation function for dense scattering media also indicate that the scatterer volume fraction at which the maximum backscatter occurs is dependent on the ultrasound frequency. Computations for 42 μm scatterers suggest that the peak value should increase with frequency in the 2–9 MHz range. Measurement results generally agreed with this prediction, as shown in Table V, column 8. An exception is the 9 MHz frequency data, where the apparent peak backscatter coefficient is at a volume fraction of around 24%, below the volume fraction for peak backscatter at 7.5 MHz. We believe this is due to experimental uncertainties, either occurring in the construction of the phantom or in measuring the backscatter coefficient. Measurement uncertainties are highest at 9 MHz, where errors in attenuation and in specifying the geometric properties of the transducer would manifest most significantly.

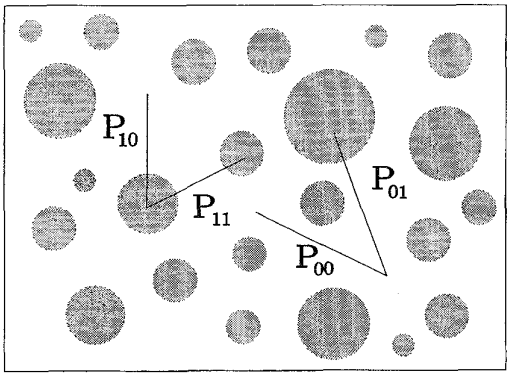

Fig. 9. For a two-component scattering medium, we consider Δr the length of a rod thrown arbitrarily into the medium. We define P_{ab} as the probability that with one end of the rod in environment a, the other end will be in environment b. Thus, four probabilities, P_{00}, P_{01}, P_{10}, P_{11} exist, where the subscript 0 stands for background material and 1 for a scatterer.

Results of this study may provide additional insight into the nature of ultrasonic scattering from tissues. Generally, sparse scattering media are implicitly assumed in relating acoustic scattering properties to tissue microstructure [3], [5], [17]. However, most tissues would appear to be better characterized as dense scattering media rather than sparsely distributed scatterers. We cannot speculate on the biomedical implications of this finding, as it is difficult at the present time to measure ultrasonic scattering in tissues accurately enough so volume fraction dependencies would have a major effect on the outcome. Nevertheless, as theoretical models for scattering in soft tissue are more fully developed, this dependency will have to be included.

Appendix

A. Debye's Spatial Autocorrelation Function [9]

As shown in (1), the spatial autocorrelation function, $b(\Delta r)$, describes the similarity of the mass density and compressibility at two positions in the scattering volume separated by the distance Δr. For a two-component medium, the development by Debye proceeds as follows [9]. We consider Δr the length of a rod thrown arbitrarily into the scattering medium as shown in Fig. 9. We define P_{ab} as the probability that with one end of the rod in environment a, the other end will be in environment b. Thus, four probabilities, P_{00}, P_{01}, P_{10}, P_{11}, exist, where the subscript "0" stands for background material and "1" for a scatterer. Between these four probabilities, three relations are immediately clear

$$P_{00} + P_{01} = 1 \tag{A-1}$$

$$P_{10} + P_{11} = 1 \tag{A-2}$$

and

$$HP_{01} = (1 - H)P_{10} \tag{A-3}$$

where (A-3) represents the two ways, equally probable, in which the rod may have its ends in different environments.

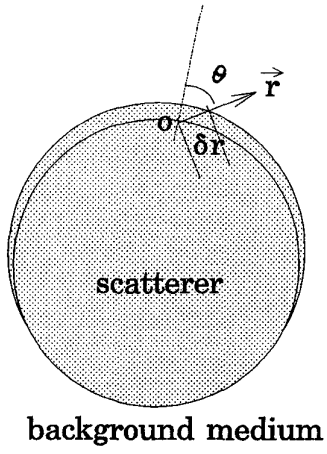

Fig. 10. For a very small δr, the value of the probability function P_{11} will change only if the addition of δr will allow Δr to cross the surface of a scatterer into the background medium or vice versa. If θ is the angle which Δr makes with respect to the normal to this surface, the free end of Δr must lie within a sheet of thickness $\delta r \cos\theta$ to allow $\Delta r + \delta r$ to cross into the background medium.

The three relations among the four probabilities allow us to express them in terms of a single arbitrary function $R(\Delta r)$ that depends on Δr. Thus, let

$$P_{01} = HR(\Delta r). \tag{A-4}$$

Notice that $P_{01} = 0$ when $\Delta r = 0$, requiring $R(\Delta r) = 0$ when $\Delta r = 0$. Then

$$P_{10} = (1 - H)R(\Delta r) \tag{A-5}$$

$$P_{11} = 1 - (1 - H)R(\Delta r) \tag{A-6}$$

and

$$P_{00} = 1 - HR(\Delta r). \tag{A-7}$$

According to the definition of the spatial autocorrelation function for a random medium, this function, $B_d(\Delta r)$, can be expressed as

$$\begin{aligned} B_d(\Delta r) &\equiv P_{10}\gamma_1\gamma_0 + P_{11}\gamma_1\gamma_1 \\ &\equiv P_{00}\gamma_0\gamma_0 + P_{01}\gamma_0\gamma_1 \\ &\equiv (1 - R(\Delta r))H^2\left(\frac{\Delta_\kappa}{\kappa} - \frac{\Delta_\rho}{\rho}\right)^2. \end{aligned}$$

The normalized spatial autocorrelation function, $b_d(\Delta r)$, can be expressed as

$$\begin{aligned} b_d(\Delta r) &\equiv \frac{B_d(\Delta r)}{B_d(0)} \\ &\equiv \frac{P_{01}\gamma_1\gamma_0 + P_{11}\gamma_1\gamma_1}{H^2\left(\frac{\Delta_\kappa}{\kappa} - \frac{\Delta_\rho}{\rho}\right)^2} \\ &= 1 - R(\Delta r). \end{aligned} \tag{A-8}$$

Let us take one point fixed in a scatterer and study how the probability function of two points that are in the same or different scatterers is affected by a change δr in Δr. For a very small Δr, the value of the probability function P_{11} will change only if the addition of δr will allow Δr to cross the surface of a scatterer into the background medium or vice versa. If θ is the angle which Δr makes with the normal to this surface, the free end of Δr must lie within a sheet of thickness $\delta r \cos\theta$ to allow $\Delta r + \delta r$ to cross into the background medium, as shown in Fig. 10. The average value of $\delta r \cos\theta$ is given by the integral (over all possible orientations)

$$\frac{\delta r}{2}\int_0^{\pi/2} \cos\theta \sin\theta d\theta = \frac{\delta r}{4}.$$

Then, we may write the change in P_{11}, δP_{11}, when Δr is changed by δr, as

$$\delta P_{11} = -\frac{S\delta r}{4V_S}P_{11} \tag{A-9}$$

where V_S = the total volume of the scatterers, S = the total surface area of the scatterers, and $S\delta r/4$ is the volume in which the free end of Δr must lie for the orientation favorable to a crossing of the scatterer–background interface. However, since it is possible that the free end of Δr is already in the background from the start, we add a second term to (A-9) for δP_{11} to account for the positive contribution that would be made to P_{11} by the growth Δr toward and into another scatterer. Then, the change in the value of the probability function P_{11}, when Δr is changed by δr, is given by

$$\delta P_{11} = -\left(\frac{S\delta r}{4V_S}\right)P_{11} + \left(\frac{S\delta r}{4V_v}\right)P_{10} \tag{A-10}$$

where V_V = the volume of the background medium. Replacing δr and δP_{11} by their differentials in the limit, we obtain

$$\frac{dP_{11}}{dr} = -\frac{SP_{11}}{4V_S} + \frac{SP_{10}}{4V_v}. \tag{A-11}$$

According to (A-4)–(A-7), we have $P_{11} = 1 - (1 - H)(1 - b_d(\Delta r))$ and $P_{10} = (1 - H)(1 - b_d(\Delta r))$. Upon substitution into (A-11), we find

$$\frac{db_d(\Delta r)}{dr} = -\frac{S}{4VH(1-H)}b_d(\Delta r) \tag{A-12}$$

where $V = V_V + V_S$. The normalized solution of this equation is given by

$$\begin{aligned} b_d(\Delta r) &= e^{-S\Delta r/[4VH(1-H)]} \\ &= e^{-3\Delta r/[4r_d(1-H)]} \end{aligned} \tag{A-13}$$

where r_d is the characteristic radius of the scatterers. If the scatterers are spherical, $S = \langle N\rangle 4\pi r_d$ and $V_S = \langle N\rangle 4\pi r_d^3/3$ where $\langle N\rangle$ is the scatterer concentration.

B. Yagi's Spatial Autocorrelation Function [10]

Concerning the results of Debye's model, Frisch noted that there were two potential problems [11]. One problem relates the incremental volume δV of (A-9) to the "sheet" of points in which the end of the rod of length Δr must lie such that if this length is increased by δr, it will cross a phase boundary. The second problem is that (A-10) neglects the possibility that more than one phase boundary may be crossed by the rod when its length is increased by δr.

In general, the spatial autocorrelation function can be approximated as the sum of N terms of the exponential functions [10]

$$b_y(\Delta r) \approx \sum_{n=1}^{N} c_n e^{-(\Delta r/a_n)^n} \tag{A-14}$$

where c_n and a_n are constants.

When Δr is small, $b_y\ (\Delta r)$ can be represented as a polynomial function based on a Taylor series expansion

$$b_y(\Delta r) \approx \sum_{n=1}^{N} c_n - \left(\frac{c_1}{a_1}\right)\Delta r + \frac{1}{2!}\left(\frac{c_1}{a_1^2} - 2\frac{c_2}{a_2^2}\right)(\Delta r)^2 + 0((\Delta r)^3). \tag{A-15}$$

Alternatively for small Δr, based on the theory of differential geometry [11], Fritsch shows that the spatial autocorrelation function can be approximated as

$$b_y(\Delta r) \approx 1 - \left(\frac{3}{4(1-H)r_y}\right)(\Delta r) + 0((\Delta r)^3) \tag{A-16}$$

where the assumption is made that scatterers are spherical with a mean radius of r_y. Retaining only the first two terms in (A-15) and comparing with (A-16), we can write

$$c_1 + c_2 = 1 \tag{A-17}$$

$$\frac{c_1}{a_1} = \frac{3}{4(1-H)r_y} \tag{A-18}$$

and

$$\frac{c_1}{a_2} = 2\left(\frac{a_1}{a_2}\right)^2. \tag{A-19}$$

For very low frequency conditions ($k \rightarrow 0$) and low scatterer concentrations ($H \rightarrow 0$), we have [10]

$$\mathrm{FT}\{b_y(\Delta r)\}|_{k\rightarrow 0,\, H\rightarrow 0} = \frac{4\pi r_y^3}{3}$$

where FT stands for the Fourier transform. Using the representation of $b_\gamma(\Delta r)$ from (A-14) along with the coefficients, this works out to

$$8\pi a_1^2\left\{c_1 + \frac{\pi^{1/2}}{8}c_2\left(\frac{a_2}{a_1}\right)^3\right\} = \frac{4\pi r_y^3}{3}. \tag{A-20}$$

From (A-17)–(A-20), we obtain [7]

$$c_1 \approx 0.40$$
$$c_2 \approx 0.60$$
$$a_1 = 0.53(1-H)r_y$$
$$a_2 = 0.92(1-H)r_y.$$

This yields a normalized spatial autocorrelation function given by

$$b_y(\Delta r) \approx 0.40e^{-\frac{\Delta r}{0.53(1-H)r_y}} + 0.60e^{-\left[\frac{\Delta r}{0.92(1-H)r_y}\right]^2}. \tag{A-21}$$

C. Uncertainty Analysis on the Frequency Dependence of the Backscatter Coefficient

The power law curves were used to fit our experimental results of the frequency dependence of the backscatter coefficient, $y(f) = af^m$, where f is the ultrasound frequency in MHz, a is a constant, and m is an index parameter for the power law.

The square of the difference between the fitting curve and the experimental data is denoted by

$$L(m) = \sum_{i=1}^{N}(y_i - y_{io})^2 \tag{A-22}$$

where N is number of the measured values of the backscatter coefficient y_{io} at different f_i, and $y_i = af_i^m$.

Under the condition of the minimum square of the difference between the values of the fitting curve and the measured values

$$F(m) = \frac{1}{2} \times \frac{\partial L(m)}{\partial m} = \sum_{i=1}^{N}(y(f_i) - y_{io})\frac{\partial y(f_i)}{\partial m} = 0$$

we have

$$F(m) = \sum_{i=1}^{N}\left(af_i^m - y_{io}\right)af_i^m \ln f_i = 0. \tag{A-23}$$

Therefore the uncertainty of the index m is given by

$$\delta m = \left\{\sum_{j=1}^{N}\left[\left(y_{jo} \times \frac{\partial m}{\partial y_{jo}}\right)^2 \times \left(\frac{\delta y_{jo}}{y_{jo}}\right)^2\right]^2\right\}^{1/2} \tag{A-24}$$

where $\delta y_{jo}/y_{jo}$ is the relative uncertainty of the measurement result for the backscatter coefficient and

$$\frac{\partial m}{\partial y_{jo}} = -\frac{(\partial F/\partial y_{jo})}{(\partial F/\partial m)} = \frac{-y_j \ln(f_j)}{\sum_{i=1}^{N}\left\{(2y_i^2 - y_i y_{io})[\ln(f_i)]^2\right\}}.$$

REFERENCES

[1] J. A. Campbell and R. C. Waag, "Normalization of ultrasonic scattering measurements to obtain average differential scattering cross sections for tissues," *J. Acoust. Soc. Amer.*, vol. 74, p. 393, 1983.

[2] M. F. Insana and D. G. Brown, "Acoustic scattering theory applied to soft biological tissue," in *Ultrasonic Scattering in Biological Tissues*, K. K. Shung and G. A. Thieme, Eds. Boca Raton, FL: CRC, 1993, pp. 75–124.

[3] M. F. Insana, T. J. Hall, and J. L. Fishback, "Identifying acoustic scattering sources in normal renal parenchyma from the anisotropy in acoustic properties," *Ultrasound Med. Biol.*, vol. 17, p. 613, 1991.

[4] F. G. Sommer, R. A. Stern, and H. Chen, "Cirrhosis: US imaging with narrow band filtering," *Radiology*, vol. 187, p. 425, 1987.

[5] F. L. Lizzi *et al.*, "Relationship of ultrasound spectral parameters for features of tissue microstructure," *IEEE Trans. Sonics Ultrason.*, vol. SU-34, p. 318, 1987.

[6] K. K. Shung, Y. W. Yuan, and D. Y. Fei, "Effect of flow disturbance on ultrasonic backscatter from blood," *J. Acoust. Soc. Amer.*, vol. 75, p. 1265, 1984.

[7] P. M. Morse and K. U. Ingard, *Theoretical Acoustics*. Princeton: Princeton Univ. Press, 1968, p. 439.

[8] J. A. Campbell and R. C. Waag, "Ultrasonic scattering properties of three random media with implication for tissue characterization," *J. Acoust. Soc. Amer.*, vol. 75, p. 1879, 1984.
[9] P. Debye, H. R. Anderson, and H. Brumberger, "Scattering by an inhomogeneous solid, II. The correlation function and its application," *J. Appl. Phys.*, vol. 28, p. 679, 1957.
[10] S. I. Yagi and K. Nakayama, "Acoustical scattering in weakly inhomogeous disperse media: Theoretical analysis," *J. Acoust. Soc. Jpn.*, vol. 36, p. 496, 1980.
[11] H. L. Frisch and F. H. Stillinger, "Contribution to the statistical geometric basis of radiation scattering," *J. Chem. Phys.*, vol. 38, p. 2200, 1963.
[12] L. Y. L. Mo and S. C. Cobbold, "Theoretical models of ultrasonic scattering in blood," in *The Book of Ultrasonic Scattering in Biological Tissues*. Boca Raton, FL: CRC, 1993.
[13] E. L. Madsen, J. A. Zagzebski, R. Banjavic, and R. E. Jutila, "Tissue-mimicking materials for ultrasound phantoms," *Med. Phys.*, vol. 5, p. 391, 1978.
[14] J. F. Chen, J. A. Zagzebski, and E. L. Madsen, "Tests of backscatter coefficient measurement using broadband pulses," *IEEE Trans. Sonics Ultrason.*, vol. 40, p. 603, 1993.
[15] E. L. Madsen, M. F. Insana, and J. A. Zagzebski, "Method of data reduction for accurate determination of acoustic backscatter coefficient," *J. Acoust. Soc. Amer.*, vol. 76, p. 913, 1984.
[16] R. R. Sokal and F. J. Rohlf, *Biometry*. San Francisco: Freeman, 1981.
[17] J. H. Rose, M. R. Kaufmann, S. A. Wickline, S. A. Hall, and J. G. Miller, "A proposed microscopic elastic wave theory for ultrasonic backscatter from myocardial tissue," *J. Acoust. Soc. Amer.*, vol. 97, p. 656, 1995.

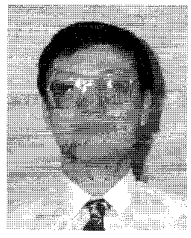

Jian-Feng Chen was born in Hangzhou, China. He received the B.S. degree in physics from Tongji University, Shanghai, China, in 1985, and the M.S. and Ph.D. degrees in medical physics from the University of Wisconsin, Madison, in 1992 and 1994, respectively.

He is a Senior Scientist at Siemens Medical Systems, Inc. His current research interests are in general medical physics and medical ultrasound.

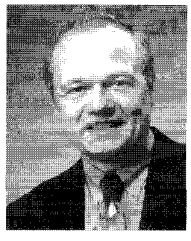

James A. Zagzebski (A'89) received the B.S. degree in physics from St. Mary's College, Winona, MN, and the M.S. degree in physics and the Ph.D. degree in radiological sciences from the University of Wisconsin, Madison.

He is a Professor of Medical Physics and of Radiology and Human Oncology at the University of Wisconsin. His research interests are quantitative ultrasound imaging, methods for assessing imaging performance of ultrasound equipment, and flow visualization using ultrasound.